Partitions for Spectral (Finite) Volume Reconstruction in the Tetrahedron

Qian-Yong Chen*

Abstract

In this paper, we compute partitions of the tetrahedron for up to the fourth-order spectral volume reconstruction. Certain optimization is made to these partitions and previously obtained partitions of lower dimensional simplex. These optimized partitions have the smallest Lebesgue constants among currently known spectral volume partitions.

*Institute for Mathematics and its Applications, University of Minnesota, Minneapolis, MN 55455 (qchen@ima.umn.edu).

1 Introduction

Spectral volume reconstruction is a key element of the recently proposed spectral volume method [9, 10] for hyperbolic conservation laws. Analogous to the well known fact that the quality of polynomial interpolation depends on the interpolation points set, the quality of spectral volume reconstruction in the simplex is determined by the partition of the simplex [3]. Since the development of the spectral volume method, some research has been done on the partition generation. For example, by following the idea of Chen and Babuška [1, 2], Wang and Liu computed the so called mean L^2 optimal partitions for up to the seventh order spectral volume reconstruction of the one-dimensional simplex [11]. Several systematic techniques based on the Voronoi diagram and its variants have also been developed in [3] for both the one and two-dimensional simplex. More recently, a linear partition and a quadratic partition of the tetrahedron were constructed in [7].

However, partitions for high order spectral volume reconstruction on the tetrahedron are still unavailable. In this paper we compute up to the fourth-order partitions of the three-dimensional simplex, S^3. These partitions are based on the idea we proposed in [3], i.e., building the partition through extensive use of the geometry structure of the interpolation points in the simplex, such as the symmetry and layering structure. The idea can be extended to generate higher order partitions of the tetrahedron. Optimization within the framework of building these partitions is also made for these partitions and the previously obtained partitions of the one and two-dimensional simplex.

Denote $\mathbf{P}^n(S^3)$ as the space of polynomials of degree up to n in three variables. The dimension of this approximation space is

$$N_n = \dim \mathbf{P}^n(S^3) = \binom{3+n}{3} = \frac{(n+1)(n+2)(n+3)}{6}.$$

$N = N_n$ and $\mathbf{P}^n = \mathbf{P}^n(S^3)$ will be used to simplify the notations if there is no confusion. Assume $\{p_1(x, y, z), \cdots, p_N(x, y, z)\}$ forms a complete basis of $\mathbf{P}^n(S^3)$.

Given any continuous function $u(x, y, z)$ on S^3, i.e., $u \in C(S^3)$, the computation of its

n-th order spectral volume reconstruction on S^3 consists of two steps:

1. Construct a partition Π_n of S^3 with N non-overlapping sub-cells (only polyhedron sub-cells are considered):

$$S^3 = C_1 \cup \cdots \cup C_N.$$

2. Find a projection $\mathcal{I}_{\Pi_n} u = \sum_{i=1}^{N} a_i \; p_i(x,y,z) \in \mathbf{P}^n$, which shares the same average as u on all the sub-cells, i.e.,

$$\frac{1}{V_i} \int_{C_i} (\mathcal{I}_{\Pi_n} u) \; dV = \frac{1}{V_i} \int_{C_i} u(x,y,z) dV, \qquad i = 1, \cdots, N, \tag{1}$$

where V_i denotes the area of sub-cell C_i.

Denote $\bar{u}_i$ as the average of $u(x,y,z)$ over sub-cell C_i, i.e.,

$$\bar{u}_i = \frac{1}{V_i} \int_{C_i} u(x,y,z) \; dV, \qquad i = 1, \cdots, N.$$

Rewrite the system (1) into a matrix form: $\mathbf{A}\mathbf{a} = \mathbf{u}$ with $\mathbf{a} = (a_1, \cdots, a_N)^T$ and $\mathbf{u} = (\bar{u}_1, \cdots, \bar{u}_N)^T$. The reconstruction matrix $\mathbf{A}$ takes the form

$$\mathbf{A} = \begin{pmatrix} \frac{1}{V_1} \int_{C_1} p_1(x,y,z) dV & \cdots & \frac{1}{V_1} \int_{C_1} p_N(x,y,z) dV \\ \cdots & \cdots & \cdots \\ \frac{1}{V_N} \int_{C_N} p_1(x,y,z) dV & \cdots & \frac{1}{V_N} \int_{C_N} p_N(x,y,z) dV \end{pmatrix}. \tag{2}$$

Assuming the reconstruction matrix is nonsingular, the projection $\mathcal{I}_{\Pi_n} u$ can be expressed in the Lagrange form, $\mathcal{I}_{\Pi_n} u = \sum_{i=1}^{N} \bar{u}_i \; L_i(x,y,z)$, where the cardinal basis functions $\mathbf{L} = (L_1, \cdots, L_N) = (p_1, \cdots, p_N) \; \mathbf{A}^{-1}$.

Then we equip the space $\mathbf{P}^n$ and $C(S^3)$ with an L^∞ norm (supremum-norm, denoted as $\|\cdot\|$) and the induced functional norm

$$\|\mathcal{I}_{\Pi_n}\| \; = \; \sup_{\|u\| \neq 0} \frac{\|\mathcal{I}_{\Pi_n} u\|}{\|u\|}.$$

Since $|\bar{u}_i| \leq \|u\|$ for $i = 1, \cdots, N$, one can show that

$$\|\mathcal{I}_{\Pi_n}\| = \max_{(x,y,z) \in S^3} \sum_{i=1}^{N} |L_i(x,y,z)| \, .$$

From the linearity of the projection operator $\mathcal{I}_{\Pi_n}$ and the fact that $\mathcal{I}_{\Pi_n} f = f, \forall f \in \mathbf{P}^n(S^3)$, it is easy to verify that the error of spectral volume reconstruction can be bounded as

$$\|u - \mathcal{I}_{\Pi_n} u\| \leq (1 + \Lambda(\Pi_n)) \, \|u - u^*\|, \tag{3}$$

where u^* is the optimal approximating polynomial whose existence is guaranteed by the continuity of $u(x, y, z)$ [4]. And

$$\Lambda(\Pi_n) = \|\mathcal{I}_{\Pi_n}\| = \max_{(x,y)\in S^3} \sum_{i=1}^{N} |L_i(x, y, z)| \tag{4}$$

is called the Lebesgue constant of the operator $\mathcal{I}_{\Pi_n}$.

According to (3), the partitions with small Lebesgue constants are preferred. It is rather difficult to directly build good high order partitions, specially for three dimensional spectral volume reconstructions, because there are too many parameters such as the position of points, the number of edges for each sub-cell and the topology of the sub-cells. For another reconstruction problem, the polynomial interpolation, several almost optimal sets have been obtained (see [8, 5, 1, 2] and reference therein). At a glimpse, it seems that the methodology of [1, 2] can be used to optimize the spectral volume partition. However, as shown in [11], the mean L^2 optimal partitions are even not very satisfactory for the one-dimensional case. So in this paper we do not compute the mean L^2 optimal partitions. Instead, we only compute partitions based on the polynomial interpolation points, and try to optimize these partitions within the framework of constructing them. In addition, we try to minimize the number of total faces of the partition whenever it is possible.

The rest of the paper includes three sections. In Sec. 2, we describe the algorithm of computing up to the fourth order partition of the tetrahedron. Section 3 is devoted to the optimization of the partitions in Sec. 2 and the partitions of the lower dimensional simplex developed in [3]. Finally we summarize the paper in Sec. 4.

2 Partitions of the Tetrahedron

In this section, we propose an algorithm to compute symmetric partitions for the spectral volume reconstruction in the tetrahedron. Similar to the technique developed in [3] for the lower dimensional simplex, this algorithm exploits the geometry structure of interpolation points on the tetrahedron (points from [6] are used in this paper). The algorithm is described in a recursive fashion in the sense of high order partitions being based on lower order partitions. In specific, when building high order partitions, we first group all the interpolation points except those on a single tetrahedron face into a new points set. Then we construct some sub-cells from the new points set with the algorithm for the one-order lower partition. We will explain it in detail in the following.

The symmetry property of the partitions is extensively used in the algorithm. But unlike polynomial interpolation, we cannot first compute the possible number of different symmetric points such as four-fold or six-fold symmetric points, as the authors did in [2]. It is because the total number of vertices for any order partition is not a fixed number, which is a direct consequence of the fact that a face can have any number (≥ 3) of vertices. For a similar reason, the total number of faces is also not a fixed number for a given order partition of the tetrahedron. So in the following, we will try to minimize, besides the Lebesgue constant, the number of faces as that is proportional to the work load of the spectral volume method [10, 9].

2.1 The First Order Partition

Our first order partition is the same as that given in [7]. But we describe our algorithm within a more general setting so that the algorithm can be used to generate higher order partitions.

Follow the idea of [3], we build the partition from the polynomial interpolation points on the tetrahedron in a certain way such that each sub-cell contains an input point. For the first order partition, the input points are simply the vertices of the tetrahedron. So a

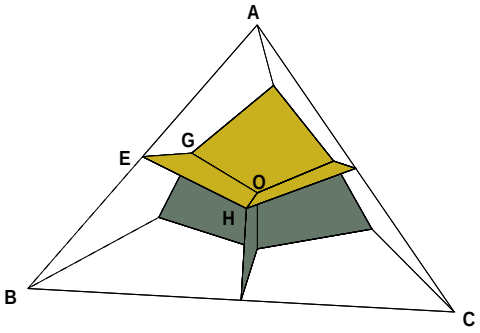

Figure 1: First order partition of the tetrahedron.

sub-cell is needed for each vertex of the tetrahedron. The four sub-cells can be computed in the exactly same way because of symmetry. Hence we only describe how to construct the sub-cell for one vertex. Figure 1 shows the sub-cell for vertex A in tetrahedron $ABCD$ (point D is behind the scene). This sub-cell consists of three interior 'faces' and three faces which are on the faces of the tetrahedron. Again by symmetry, the three interior faces can be constructed in a similar way. One such interior face is $EHOG$, in which O is inside the tetrahedron, E is on the edge AB, and G and H are on the face ABD and ABC respectively. In this face, we require that point G has the same barycenter coordinates in ΔABD as the point H in ΔABC. Moreover, as shown in Fig. 1, the three remaining faces will be fixed after building the interior faces. So it suffices to specify how to choose points O, E and G, in order to compute the sub-cell for vertex A, thus the whole first order partition. In the following, bold symbols represent the coordinates of points in column vector form.

Note that the points E, H, O and G are not always coplanar. We choose the points O, E and G with form

$$\begin{cases} \mathbf{O} & = r\ \mathbf{B} + r\ \mathbf{C} + r\ \mathbf{D} + (1-3r)\ \mathbf{A}, \\ \mathbf{E} & = s\ \mathbf{B} + (1-s)\ \mathbf{A}, \\ \mathbf{G} & = t\ \mathbf{B} + t\ \mathbf{D} + (1-2t)\ \mathbf{A}, \end{cases} \tag{5}$$

where $0 < r, s, t < 1$. For the first order partition, we have $r = 1/4, s = 1/2$ and $t = 1/3$ according to the symmetry property. So O, E and G are the mass center of the tetrahedron

$ABCD$, edge AB and face ABD respectively. The partition consists of four hexahedrons, each of which has six quadrilateral faces as shown in Fig. 1. (From **Lemma** 1, one can verify that the points O, G, E and H are coplanar.) The data set of the partition is given in Table 1-3. The Lebesgue constant for such partition is 95/26 (see [7]).

Lemma 1 *The points O, G, E and H are coplanar if and only if $(st + rt - 2rs) = 0$.*

Proof: According to symmetry, $\mathbf{H} = t\ \mathbf{B} + t\ \mathbf{C} + (1 - 2t)\ \mathbf{A}$. So

$$(\mathbf{O}\quad \mathbf{G}\quad \mathbf{E}\quad \mathbf{H}) = (\mathbf{A}\quad \mathbf{B}\quad \mathbf{C}\quad \mathbf{D}) \begin{pmatrix} 1-3r & 1-2t & 1-s & 1-2t \\ r & t & s & t \\ r & 0 & 0 & t \\ r & t & 0 & 0 \end{pmatrix}.$$

The points O, G, E and H are coplanar if and only if the above matrix is singular. The determinant of the above matrix is equal to $t(st + rt - 2rs)$, which finishes the proof. ■

2.2 The Second Order Partition

Second-order polynomial interpolation on the tetrahedron needs ten interpolation points. We choose four tetrahedron vertices and six tetrahedron edge middle points as the interpolation points (see Fig. 2). For the four tetrahedron vertices, we construct a sub-cell for each of them as we did for the first order partition in the last section. For example, when building the sub-cell for vertex A, we treat A as a vertex of a small tetrahedron $AIJH$ (Fig. 2), and employ the algorithm described in the last section to construct the sub-cell containing A. Note that the three parameters r, s and t are not constant this time. We consider only the parameters which ensure that each of these four sub-cells has six quadrilateral faces (i.e., condition of **Lemma** 1 is satisfied). In Sec. 3.3, we will vary r, s, t with the above constraint to minimize the Lebesgue constant of the partition.

For the six remaining points, it is enough to explain how to compute the sub-cell for one point (e.g., point I) as we will build the other five sub-cells in a symmetric way. In our second order partition, the sub-cell (Fig. 2) for point I has eight faces: two quadrilateral faces, two pentagon faces, and four more symmetric quadrilateral 'faces'. Among those faces,

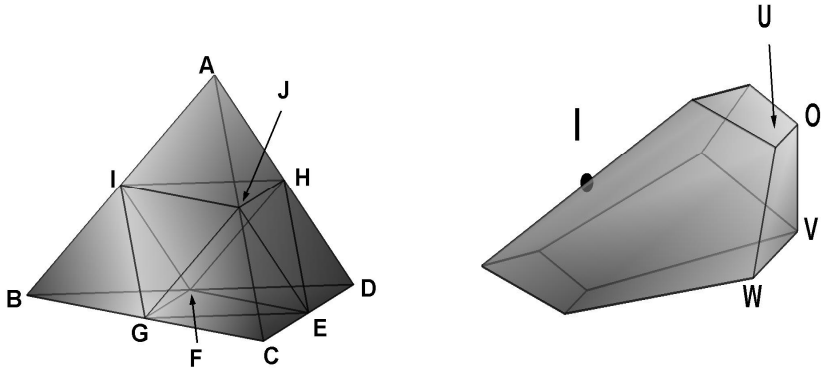

Figure 2: The second order partition. Left: a tetrahedron with input points; Right: the sub-cell that includes point I.

the two quadrilateral faces also separately belong to the sub-cell including point A and B. The two pentagon faces are on the tetrahedron face ABC and ABD respectively, and they will be fixed after building the four symmetric faces. In Fig. 2, we mark one of these four faces as $UOVW$. In this face, the point U is also on the triangle face AIJ, and O is inside the small tetrahedron $AIJH$. In fact, these two points have already been specified when building the sub-cell for vertex A. So the only remaining work is to choose points W and V. We put point W inside the triangle IJG and V inside the octahedron $IJHEFG$. In particular, we choose

$$\begin{cases} \mathbf{W} & = \frac{\mathbf{I}+\mathbf{J}+\mathbf{G}}{3}, \\ \mathbf{V} & = \frac{\mathbf{I}+\mathbf{J}+\mathbf{G}+\mathbf{E}+\mathbf{H}+\mathbf{F}}{6}, \\ \mathbf{O} & = r\ \mathbf{I} + r\ \mathbf{J} + r\ \mathbf{H} + (1-3r)\ \mathbf{A}, \\ \mathbf{U} & = t\ \mathbf{I} + t\ \mathbf{J} + (1-2t)\ \mathbf{A}, \end{cases} \tag{6}$$

where the specification of O and U are also included for completeness. These four points always form a quadrilateral according to the following lemma.

Lemma 2 *The four points, $W, V, O,$ and U as defined in* (6)*, are always coplanar.*

Proof: According to the distribution of the input points, there exists λ, η such that

$$\begin{cases} \mathbf{I} & = \lambda\ \mathbf{A} + (1-\lambda)\ \mathbf{B}, & \mathbf{G} = \eta\ (\mathbf{B}+\mathbf{C}) + (1-2\eta)\mathbf{A}, \\ \mathbf{J} & = \lambda\ \mathbf{A} + (1-\lambda)\ \mathbf{C}, & \mathbf{E} = \eta\ (\mathbf{C}+\mathbf{D}) + (1-2\eta)\mathbf{A}, \\ \mathbf{H} & = \lambda\ \mathbf{A} + (1-\lambda)\ \mathbf{D}, & \mathbf{F} = \eta\ (\mathbf{B}+\mathbf{D}) + (1-2\eta)\mathbf{A}. \end{cases} \tag{7}$$

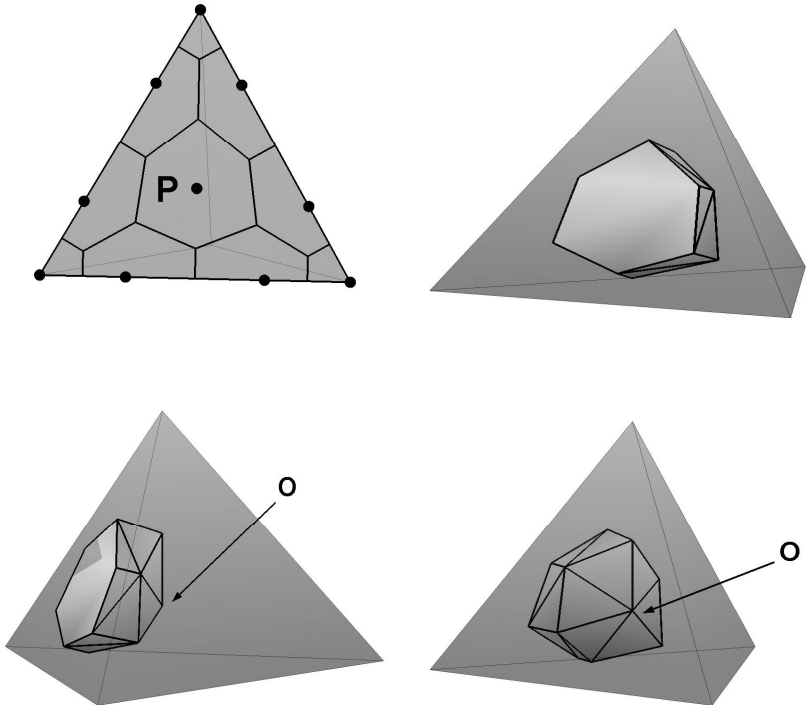

Figure 3: The third order partition of the tetrahedron: a sub-cell.

Substitute the above formula into (6) to obtain

$$(\mathbf{U}\quad\mathbf{O}\quad\mathbf{W}\quad\mathbf{V}) = (\mathbf{A}\quad\mathbf{B}\quad\mathbf{C}\quad\mathbf{D}) \begin{pmatrix} 1-2t+2t\lambda & 1-3r+3r\lambda & \frac{1-2\eta+2\lambda}{3} & \frac{3+3\lambda-6\eta}{6} \\ t(1-\lambda) & r(1-\lambda) & \frac{1+\eta-\lambda}{3} & \frac{1-\lambda+2\eta}{6} \\ t(1-\lambda) & r(1-\lambda) & \frac{1+\eta-\lambda}{3} & \frac{1-\lambda+2\eta}{6} \\ 0 & r(1-\lambda) & 0 & \frac{1-\lambda+2\eta}{6} \end{pmatrix}.$$

The matrix in the above is singular, which proves the lemma. ■

Remark 1 *For the points which are used to compute the second order partition in this section, one have* $\lambda = 1/2, \eta = 1/3$. *These special values for* λ *and* η *are not used in the proof. So the lemma also applies to certain faces of the third and fourth-order partitions which are generated with the algorithm in this section.*

2.3 The Third Order Partition

To compute the third order partition, we choose the interpolation points from [6]. All these points are on the surface of the tetrahedron. In the upper left part of Fig. 3, we plot the

points which are on one tetrahedron face. Using the algorithm to compute the second order partition, a sub-cell can be constructed for all the points shown in the picture except P. For example, when building sub-cells for the three points on the top of the picture, we ignore all the interpolation points on the lowest layer (i.e., the ten points on the bottom tetrahedron face). Then the number of remaining points will be ten, which is exactly the number of second order interpolation points. Treat these ten points as the input points and use the algorithm in Sec. 2.2 to construct the sub-cells for the three top points shown in the picture. Similar procedure can be done for all other points except P.

So the only additional work is to build a sub-cell containing point P for each tetrahedron face. We compute these four sub-cells as follows. Observing that a single connected volume will be left after excluding those sub-cells which have already been built, we choose the mass center of the original tetrahedron as a new vertex, and then connect this new vertex to certain vertices of the single volume to divide it into four identical sub-cells. One of such sub-cell is shown in Fig. 3. In the upper right, it shows a view from the side with point P. In the lower left, it is a view after rotating the tetrahedron from right to left for a small angle, where point O is the mass center of the tetrahedron. Finally in the lower right, we rotate it a little more to show the sub-cell from the opposite side. This sub-cell has one hexagonal face and 18 triangular faces. Till now we have computed a third order partition of the tetrahedron. In Sec. 3.3, we will optimize the partition by moving the input points around.

2.4 The Fourth Order Partition

The fourth order interpolation points set [6] has 35 points, only one of which is inside the tetrahedron. Figure 4 shows the points which are on one face of the tetrahedron. For each surface point, a sub-cell can be constructed with the algorithm for the third-order partition. For example, for the six points shown in the top left of Fig. 4, we can simply apply the algorithm for the third-order partition on the points set which includes all the

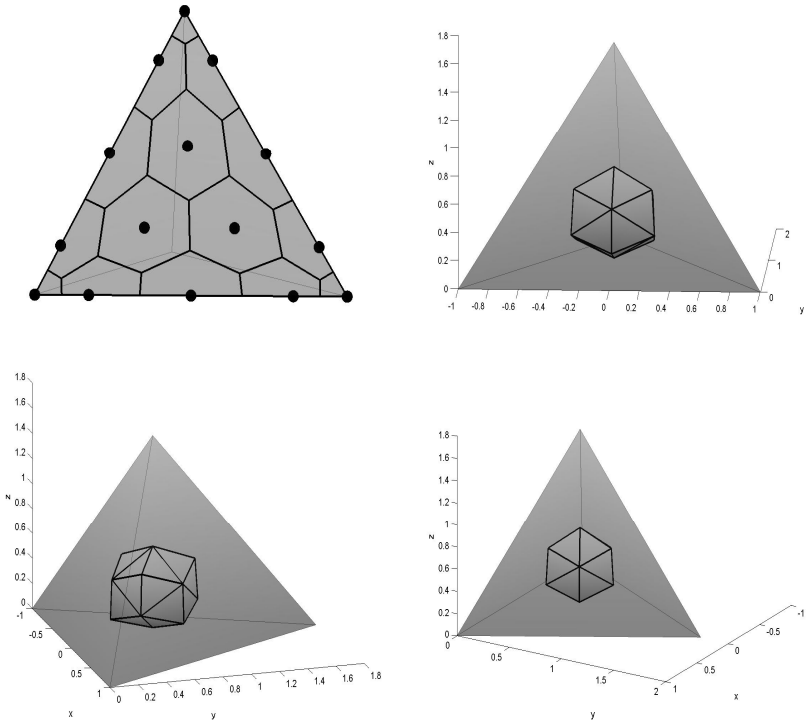

Figure 4: The interior sub-cell of the fourth order partition of the tetrahedron.

original interpolation points except those on the bottom tetrahedron face. So it seems that we only need a new technique to construct a sub-cell for the interior point. However, even this new technique is not necessary because after building all the other sub-cells, there will be left a single connected volume which is just the sub-cell for the interior point. Figure 4 shows this sub-cell from different perspective. On the top right, it is a view from the reader's side. The bottom left shows a view after rotating the tetrahedron from right to left for a certain angle. The bottom right is another view after further rotation. This sub-cell has 24 triangular faces. In Sec. 3.3, we will optimize the partition.

Remark 2 *The recursive algorithm can be used to compute higher order partitions of the tetrahedron.*

3 Partition Optimization

In this section, we optimize the partitions given in [3] and the three-dimensional partitions computed in Sec.2.

3.1 One Dimensional Partitions

In [3], we developed several one-dimensional partitions from the Chebyshev and Legendre Gauss-Lobatto points by using middle points of two neighboring input points as partition vertices. However, those partitions have larger Lebesgue constants than the partitions given in [11].

So in this paper, instead of simply using middle points of two neighboring input points as endpoints of sub-cells, we construct a partition in which most input points sit at the center of the sub-cells and the sub-cells have increasing size from the boundary to the interior. In specific, consider an even order partition with input points $-1 = x_0 < x_1 < \cdots < x_{2n} = 1$. Take $d_i = x_i - x_{i-1}, i = 1, \cdots, 2n$. Assume r be the portion of interval $[x_{n-1}, x_n]$ that is allocated to the sub-cell including x_n. So the $(1-r)d_n$ of $[x_{n-1}, x_n]$ is allocated to the sub-cell x_{n-1}, i.e., $y_n = x_{n-1} + (1-r)d_n$ is a vertex of the partition. In order to make x_{n-1} be the center of a sub-cell, $y_{n-1} = x_{n-1} - (1-r)d_n$ should also be a vertex of the partition. Hence $(1-r)d_n$ of the interval $[x_{n-2}, x_{n-1}]$ is allocated to the sub-cell including x_{n-1}. Since we require the sub-cells closer to the middle have larger size, one can have

$$\begin{cases} rd_n \geq (1-r)d_n \\ (1-r)d_n \geq \frac{d_{n-1}}{2} \end{cases} \qquad \Longrightarrow \qquad 1 - \frac{d_{n-1}}{2d_n} \geq r \geq \frac{1}{2}.$$

Continue the above process until we get y_0 such that x_0 is the middle point of $[y_0, y_1]$. Repeat it for the other half interpolation points, $\{x_{n+1}, \cdots, x_{2n}\}$, to get the whole partition. Note that the partition will cover a region larger than the original domain $[-1, 1]$. A partition of $[-1, 1]$ can be easily obtained by a linear mapping. Similar procedure can be done for odd order partitions.

In the algorithm, r is the only parameter to be optimized. With the above algorithm,

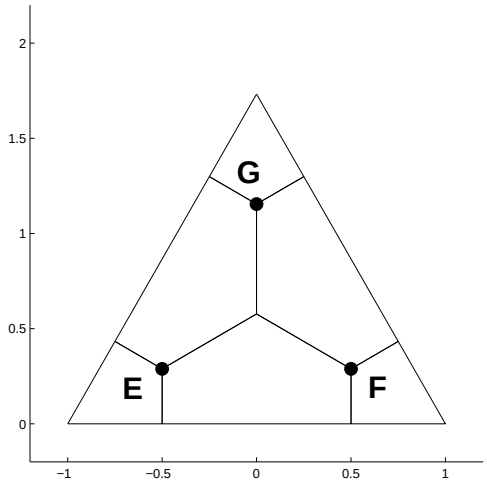

Figure 5: The second order partition of the triangle.

we compute the optimal partitions from the Legendre-Gauss-Lobatto, Chebyshev-Gauss-Lobatto points, and the optimal polynomial interpolation set [1]. These optimized partitions are denoted as Π_{LGL}, Π_{CGL}, and Π_{T_1} respectively, among which Π_{LGL} is the smallest for partitions of most order. The results are shown in Tab. 4-5.

3.2 Two Dimensional Partitions

We only optimize the partitions of up to the fourth order in the triangle which are given in [3]. Different constraint will be applied when optimizing partitions of different order.

3.2.1 The Second Order Partition of the Triangle

Figure 5 shows the second order partition from [3]. We seek an optimal partition whose vertices on each triangle edge are just the vertices of the one-dimensional second-order partition computed in Sec. 3.1. So only three vertices of the partition, points E, F, G, are not fixed. Because of symmetry, points E, F, G are determined by a single parameter. Specially, their barycenter coordinates can be expressed as $(r, r, 1-2r), (r, 1-2r, r), (1-2r, r, r)$. Under the above constraint, the optimal partition (Fig. 6) has Lebesgue constant 3.0630, and the partition data is listed in Tab. 6-7. We also tried to move around the partition vertices which are on the triangle edges. There is little difference in the optimal Lebesgue constant.

3.2.2 The Third Order Partition of the Triangle

In [3], we propose a technique to compute the partitions from the layering structure of the input points. In that algorithm, we first generate a triangulation from the input points. The centroids of the triangles in the triangulation are then used as the vertices of the partition. (See [3] for further details.) Here we apply the same algorithm to compute the third order partition except that a different point instead of the centroid in each triangle is chosen to be a vertex of the partition. In particular, we choose a weighted average of the triangle vertices, with the weight being the largest barycenter coordinate of each triangle vertex. Within the above algorithm, we move around the input points while keeping its symmetry property to obtain a partition with the smallest Lebesgue constant. The optimal partition obtained this way is shown in Fig. 6, and its Lebesgue constant is 3.2129. The partition data is given in Tab.8-9. We also tried to compute the optimal partition under the constraint similar to Sec. 3.2.1. The result is not as good as the one we give here.

3.2.3 The Fourth Order Partition of the Triangle

For the fourth order partition, we follow the similar idea of Sec. 3.2.1, i.e., using the optimal one-dimensional partition from Sec. 3.1 on the edge of triangle, and then moving around the other partition vertices to get a small Lebesgue constant. The partition shown in Fig. 6 has Lebesgue constant 4.0563. Note that this partition is not optimal. But when perturbing the partition vertices, only a few percent change is observed in the Lebesgue constant. The partition data is given in Tab. 10-11.

3.3 The Three Dimensional Partitions

For the second order partition, we use the optimized second order partition of the triangle computed in Sec. 3.2.1 on the faces of the tetrahedron. In order to minimize the number of total faces, the partition vertices inside the tetrahedron are chosen such that the condition of **Lemma** 1 is satisfied. Then the partition is actually fixed, which is shown in Fig. 7. The

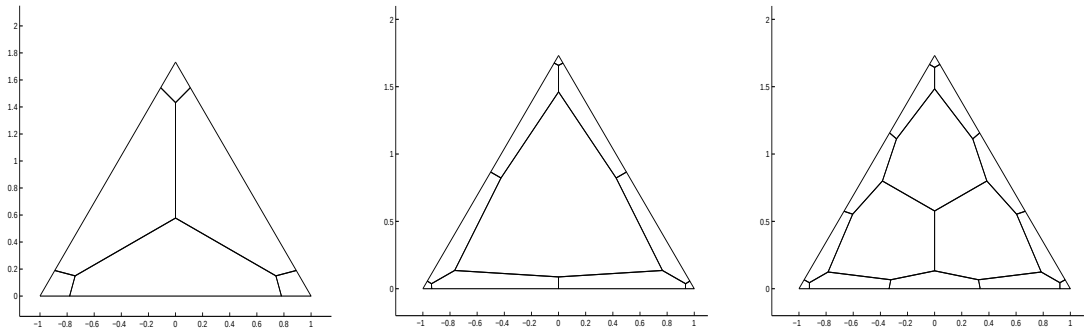

Figure 6: Several two-dimensional partitions. Left: second order; Middle: third order; Right: fourth order.

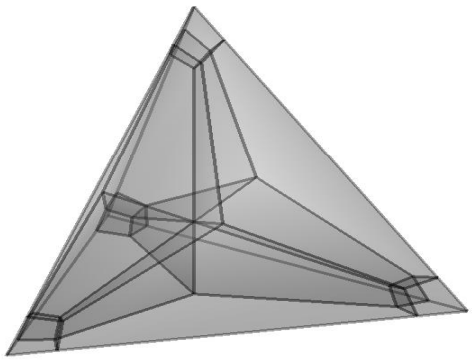

Figure 7: Second order partition of tetrahedron.

partition has 37 vertices and 48 faces, and its Lebesgue constant is 5.0814.

For the third and fourth order partitions, we simple employ the algorithm given in Sec. 2.3 and 2.4 to compute the partition, and try to find the one with minimal Lebesgue constant by moving the input points around. The smallest Lebesgue constants we found for the third and fourth order partitions are 6.8725 and 7.9940 respectively. The obtained third order partition has 73 vertices and 130 faces, while the fourth order partition has 126 vertices and 252 faces. Note that this fourth order partition has some non-convex sub-cells.

The data for the second, third, and fourth-order partitions are not included in the paper as large tables are needed to describe them. All the partitions in the paper can be downloaded from the author's homepage at "http://www.ima.umn.edu/∼qchen".

4 Conclusions

We have computed the partitions of up to the fourth order for the tetrahedron. The partitions are constructed in a hierarchy way so that higher order partitions are based on lower order partitions. Therefore, when building a certain order partition, we only need to specify how to construct one particular type of sub-cells as all other sub-cells can be obtained in the way generating the one order lower partition.

Optimization within the framework of generating the partitions are also made to both the partitions of tetrahedron obtained in this paper and the previously reported partitions for lower dimensional simplex. The resulted partitions have the smallest Lebesgue constant among the currently known partitions.

Appendix A

Table 1: The first order partition of the tetrahedron: the barycenter coordinates of the vertices.

i				
1	0.0000000000	0.0000000000	1.0000000000	0.0000000000
2	0.0000000000	0.0000000000	0.5000000000	0.5000000000
3	0.0000000000	0.5000000000	0.5000000000	0.0000000000
4	0.0000000000	0.3333333333	0.3333333333	0.3333333333
5	0.0000000000	1.0000000000	0.0000000000	0.0000000000
6	0.0000000000	0.5000000000	0.0000000000	0.5000000000
7	0.0000000000	0.0000000000	0.0000000000	1.0000000000
8	0.2500000000	0.2500000000	0.2500000000	0.2500000000
9	0.3333333333	0.3333333333	0.3333333333	0.0000000000
10	0.3333333333	0.0000000000	0.3333333333	0.3333333333
11	0.3333333333	0.3333333333	0.0000000000	0.3333333333
12	0.5000000000	0.5000000000	0.0000000000	0.0000000000
13	0.5000000000	0.0000000000	0.5000000000	0.0000000000
14	0.5000000000	0.0000000000	0.0000000000	0.5000000000
15	1.0000000000	0.0000000000	0.0000000000	0.0000000000

Table 2: The first order partition of the tetrahedron: the faces. Each row lists the indices of vertices for one face. M denotes the number of vertices of each individual face.

i	M				
1	4	9	13	15	12
2	4	10	14	15	13
3	4	11	14	15	12
4	4	8	11	14	10
5	4	8	11	12	9
6	4	8	10	13	9
7	4	1	13	10	2
8	4	1	13	9	3
9	4	1	3	4	2
10	4	3	9	8	4
11	4	2	10	8	4
12	4	3	5	6	4
13	4	5	12	11	6
14	4	3	9	12	5
15	4	4	8	11	6
16	4	6	11	14	7
17	4	2	7	6	4

Table 2 (Contd.)

i	M				
18	4	2	10	14	7

Table 3: The first order partition of the tetrahedron: the sub-cells. Each row lists the indices of faces of one sub-cell. M denotes the number of faces of each individual sub-cell.

i	M						
1	6	1	2	3	4	5	6
2	6	7	8	9	10	11	6
3	6	12	13	14	5	10	15
4	6	16	17	18	11	4	15

Table 4: Lebesgue constants for several one-dimensional partitions.

order	Π_{LGL}	r	Π_{CGL}	r	Π_{T_1}	r
2	1.685	0.877	1.685	0.877	1.685	0.877
3	1.823	0.884	1.823	0.872	1.823	0.890
4	1.950	0.533	2.132	0.656	2.674	0.500
5	2.108	0.562	2.416	0.542	2.337	0.500
6	2.291	0.542	2.560	0.500	2.241	0.593
7	2.449	0.554	2.666	0.500	2.387	0.602
8	2.545	0.514	2.834	0.571	3.898	0.500
9	2.644	0.521	3.015	0.518	3.514	0.500
10	2.748	0.512	3.105	0.500	3.190	0.541
11	2.840	0.519	3.180	0.500	2.920	0.552
12	2.918	0.509	3.268	0.534	4.711	0.500
13	2.991	0.511	3.384	0.509	4.343	0.500
14	3.063	0.504	3.450	0.500	4.020	0.522
15	3.124	0.507	3.509	0.500	3.738	0.529
16	3.190	0.507	3.571	0.519	5.312	0.500
17	3.248	0.507	3.653	0.505	4.969	0.500
18	3.303	0.500	3.705	0.500	4.661	0.513
19	3.354	0.505	3.753	0.500	4.384	0.519
20	3.404	0.507	3.801	0.512		

Table 5: Node sets of the partitions Π_{LGL}. Only positive interior points are listed.

order	x_i
2	0.7812757765
3	0.8797040574

Table 5 (Contd.)

order	x_i
4	0.3358143267
	0.9232452092
5	0.5414344225
	0.9518023783
6	0.2485522653
	0.6680769262
	0.9550635604
7	0.4131856053
	0.7482430030
	0.9628667435
8	0.1837943613
	0.5315587191
	0.8025200275
	0.9700321565
9	0.3247408153
	0.6207881103
	0.8408055127
	0.9784046134
10	0.1498237400
	0.4354893164
	0.6831261231
	0.8693871112
	0.9790260552

Table 6: The second order partition of the triangle: the barycenter coordinates of the vertices.

i			
1	1.0000000000	0.0000000000	0.0000000000
2	0.8906378883	0.1093621117	0.0000000000
3	0.8269977508	0.0865011246	0.0865011246
4	0.8906378883	0.0000000000	0.1093621117
5	0.1093621117	0.8906378883	0.0000000000
6	0.0865011246	0.8269977508	0.0865011246
7	0.3333333334	0.3333333334	0.3333333331
8	0.0865011246	0.0865011246	0.8269977508
9	0.1093621117	0.0000000000	0.8906378883
10	0.0000000000	1.0000000000	0.0000000000
11	0.0000000000	0.8906378883	0.1093621117
12	0.0000000000	0.1093621117	0.8906378883
13	0.0000000000	0.0000000000	1.0000000000

Table 7: The second order partition of the triangle: the sub-cells. Each row lists the indices of vertices in counterclockwise direction for one sub-cell. M denotes the number of vertices of each individual face.

i	M					
1	4	9	8	12	13	
2	5	4	3	7	8	9
3	5	8	7	6	11	12
4	4	1	2	3	4	
5	5	3	2	5	6	7
6	4	6	5	10	11	

Table 8: The third order partition of the triangle: the barycenter coordinates of the vertices.

i			
1	0.9574919119	0.0212540441	0.0212540441
2	0.4747800545	0.4747800545	0.0504398910
3	0.8437475098	0.0781262451	0.0781262451
4	0.4747800545	0.0504398911	0.4747800544
5	0.0212540441	0.9574919119	0.0212540441
6	0.0781262451	0.8437475098	0.0781262451
7	0.0504398911	0.4747800545	0.4747800544
8	0.0781262451	0.0781262451	0.8437475097
9	0.0212540441	0.0212540441	0.9574919119
10	1.0000000000	0.0000000000	0.0000000000
11	0.0000000000	0.0000000000	1.0000000000
12	0.0000000000	1.0000000000	0.0000000000
13	0.9673771699	0.0326228301	0.0000000000
14	0.5000000000	0.5000000000	0.0000000000
15	0.0326228301	0.9673771699	0.0000000000
16	0.9673771699	0.0000000000	0.0326228301
17	0.5000000000	0.0000000000	0.5000000000
18	0.0326228301	0.0000000000	0.9673771699
19	0.0000000000	0.9673771699	0.0326228301
20	0.0000000000	0.5000000000	0.5000000000
21	0.0000000000	0.0326228301	0.9673771699

Table 9: The third order partition of the triangle: the sub-cells.

i	M					
1	4	10	13	1	16	
2	5	1	13	14	2	3
3	5	16	1	3	4	17
4	5	2	14	15	5	6

Table 9 (Contd.)

i	M						
5	6	4	3	2	6	7	8
6	5	17	4	8	9	18	
7	4	5	15	12	19		
8	5	7	6	5	19	20	
9	5	9	8	7	20	21	
10	4	11	18	9	21		

Table 10: The fourth order partition of the triangle: the barycenter coordinates of the vertices.

i			
1	1.0000000000	0.0000000000	0.0000000000
2	0.9616226046	0.0383773954	0.0000000000
3	0.9488301395	0.0255849303	0.0255849303
4	0.9616226046	0.0000000000	0.0383773954
5	0.6679071634	0.3320928367	0.0000000000
6	0.6422746261	0.3193479785	0.0383773954
7	0.8568233902	0.0715883049	0.0715883049
8	0.6422746261	0.0383773954	0.3193479785
9	0.6679071634	0.0000000000	0.3320928367
10	0.3320928367	0.6679071634	0.0000000000
11	0.3193479785	0.6422746261	0.0383773954
12	0.4616226046	0.4616226046	0.0767547908
13	0.3333333334	0.3333333334	0.3333333331
14	0.4616226046	0.0767547908	0.4616226046
15	0.3193479785	0.0383773954	0.6422746261
16	0.3320928367	0.0000000000	0.6679071634
17	0.0383773954	0.9616226046	0.0000000000
18	0.0255849303	0.9488301395	0.0255849303
19	0.0715883049	0.8568233902	0.0715883049
20	0.0383773954	0.6422746261	0.3193479785
21	0.0767547908	0.4616226046	0.4616226046
22	0.0383773954	0.3193479785	0.6422746261
23	0.0715883049	0.0715883049	0.8568233902
24	0.0255849303	0.0255849303	0.9488301395
25	0.0383773954	0.0000000000	0.9616226046
26	0.0000000000	1.0000000000	0.0000000000
27	0.0000000000	0.9616226046	0.0383773954
28	0.0000000000	0.6679071634	0.3320928367
29	0.0000000000	0.3320928367	0.6679071634
30	0.0000000000	0.0383773954	0.9616226046
31	0.0000000000	0.0000000000	1.0000000000

Table 11: The fourth order partition of the triangle: the sub-cells.

i	M						
1	4	25	24	30	31		
2	5	16	15	23	24	25	
3	5	24	23	22	29	30	
4	5	9	8	14	15	16	
5	6	14	13	21	22	23	15
6	5	22	21	20	28	29	
7	5	4	3	7	8	9	
8	6	7	6	12	13	14	8
9	6	13	12	11	19	20	21
10	5	20	19	18	27	28	
11	4	1	2	3	4		
12	5	2	5	6	7	3	
13	5	6	5	10	11	12	
14	5	10	17	18	19	11	
15	4	18	17	26	27		

References

[1] Q. Chen and I. Babuška. Approximate optimal points for polynomial interpolation of real functions in an interval and in a triangle. *Computer Methods in Applied Mechanics and Engineering*, 128:405–417, 1995.

[2] Q. Chen and I. Babuška. The optimal symmetrical points for polynomial interpolation of real functions in the tetrahedron. *Computer Methods in Applied Mechanics and Engineering*, 137:89–94, 1996.

[3] Q.-Y. Chen. Partitions of a simplex leading to accurate spectral (finite) volume reconstruction. *SIAM Journal on Scientific Computing*. To Appear.

[4] P. J. Davis. *Interpolation and Approximation*. Dover Publications, New York, 1975.

[5] J. S. Hesthaven. From electrostatics to almost optimal nodal sets for polynomial interpolation in a simplex. *SIAM Journal on Numerical Analysis*, 35(2):655–676, 1998.

[6] J. S. Hesthaven and C. H. Teng. Stable spectral methods on tetrahedral elements. *SIAM Journal on Scientific Computing*, 21(6):2352–2380, 2000.

[7] Y. Liu, M. Vinokur, and Z. J. Wang. Three-dimensional high-order spectral finite volume method for unstructured grids. In *Proceedings of 16th AIAA CFD Conference*, Orlando, Florida, 2003. AIAA Paper No. 2003-3837.

[8] M. A. Taylor, B. A. Wingate, and R. E. Vincent. An algorithm for computing fekete points in the triangle. *SIAM Journal On Numerical Analysis*, 38(5):1707–1720, 2000.

[9] Z. J. Wang. Spectral (finite) volume method for conservation laws on unstructured grids: Basic formulation. *Journal of Computational Physics*, 178:210–251, 2002.

[10] Z. J. Wang and Y. Liu. Spectral(finite) volume method for conservation laws on unstructured grids. *Journal of Computational Physics*, 179:665–697, 2002.

[11] Z. J. Wang and Y. Liu. Spectral (finite) volume method for conservation laws on unstructured grids iii: One dimensional systems and partition optimization. *Journal of Scientific Computing*, 20(1):137–157, 2004.